PERFORMANCE OF IMAGE ANALYSIS FOR ASSESSMENT OF SIMULATED SPRAY DROPLET DISTRIBUTION

M. Salyani, R. D. Fox

ABSTRACT. *Various distribution patterns of spray droplets were simulated with Autosketch V.2 software and images of specks were printed on a Laserjet 2 printer. The specks were studied with a Dapple Systems image analyzer and Imageplus+ software. The objectives were to evaluate the utility of image analysis for spray deposition assessment and determine the effects of image area, speck size, and number of specks on the accuracy of the measurements.*

The size of the image area, speck size, and the number of specks had significant effects on area coverage measurement. The accuracy of image analysis decreased as image area or speck size decreased or speck number increased. Image partitioning adversely affected the accuracy of the measurements. ***Keywords.*** *Autosketch, Laserjet, Imageplus, Pixel.*

In most pesticidal applications, the pattern of spray distribution and the uniformity of coverage directly relate to the efficiency of spraying and efficacy of pest control. Therefore, different methodologies have been used to evaluate spray deposition. Staniland (1959), Edwards et al. (1961), and Salyani and McCoy (1989) used fluorescent tracers and visually evaluated spray coverage. Ware et al. (1969), Yates et al. (1974), and Byers et al. (1984) used gas chromatography or atomic absorption spectrophotometry to quantify pesticide residues on plant surfaces. Salyani and Whitney (1988) compared fluorometry and colorimetry on leaf and mylar targets. Because these methodologies were either too subjective or were too time-consuming and expensive, several researchers attempted to automate the process and increase the accuracy and speed of spray deposition assessment.

Liljedahl and Strait (1959), Whitney and Roth (1985), and Carlton and Bouse (1988) developed instruments for a continuous measurement of spray deposition across an aerial application swath. Salyani and Serdynski (1990) and Maze and Parekh (1993) developed sensors for real-time measurement of spray deposition. Machine vision or image analysis has also been widely used in many applications. Brazee et al. (1968), Sistler et al. (1982), Kranzler and Downs (1986), Panneton (1989), and Franz (1990) developed various imaging systems that could provide somewhat detailed information about dry particle or spray droplet deposition and distribution. The size and number of the specks on the target surface and percentage of the area coverage were among several parameters that were determined with the imaging systems.

Sistler et al. (1982) found that the accuracy of the measurements were dependent on calibration of the system. Also, increasing the image size reduced the variations in readings, but decreased the accuracy of droplet size measurements. Panneton (1989) found that the fluctuations of the light intensity in time and location of the target spot in the field of view can be sources of error in measurements. Franz (1992) looked at the effects of operator subjectivity, spot size, and color contrast on the performance of his spray coverage analyzer. He did not find unique combination of contrast and spot size values that would serve as a standard for setting grey level thresholds for all combination of variables.

The literature revealed that image analysis has intrinsic limitations which may result in erroneous measurements in certain applications. The objectives of this study were to:

- Evaluate the utility of image analysis for assessment of spray deposition and distribution.
- Determine the effects of the speck size, number of specks, and image area on the accuracy of the measurements.

MATERIALS AND METHODS

DROPLET IMAGES

Various distribution patterns of spray droplets were simulated with Autosketch V.2 software (Autodesk, Inc., Sausalito, CA 94965); droplet images were printed as black specks using a 300 dpi Laserjet 2 printer (Hewlett Packard Co., Boise, ID 83714). Three sets of images were prepared.

1. Single speck images. This set consisted of thirty 1-cm^2 images, each with a single speck located at its center. The nominal size (diameter) of the specks increased from 50 to 1000 μm (in 50-μm steps) and from 1000 to 2000 μm (in 100-μm steps).
2. Mixed-speck images. This set included 10 mixed-speck images, having nominally identical distribution patterns, but printed in 1 to 10 cm squares (fig. 1, A through J). Each image contained a total of 629 specks which were made of a combination of 13

Article was submitted for publication in October 1993; reviewed and approved for publication by the Power and Machinery Div. of ASAE in June 1994. Presented as ASAE Paper No. 93-1001.

Florida Agricultural Experiment Station Journal Series No. R-03436.

Product and company names used in this article are for providing specific information only. Their mention does not imply an endorsement or recommendation over others not mentioned.

The authors are **Masoud Salyani**, ***ASAE Member Engineer***, Associate Professor, Agricultural Engineering, University of Florida, IFAS, Citrus Research and Education Center, Lake Alfred; and **Robert D. Fox**, ***ASAE Member Engineer***, Agricultural Engineer, USDA-Agricultural Research Service, Application Technology Research Unit, OARDC, Wooster, Ohio.

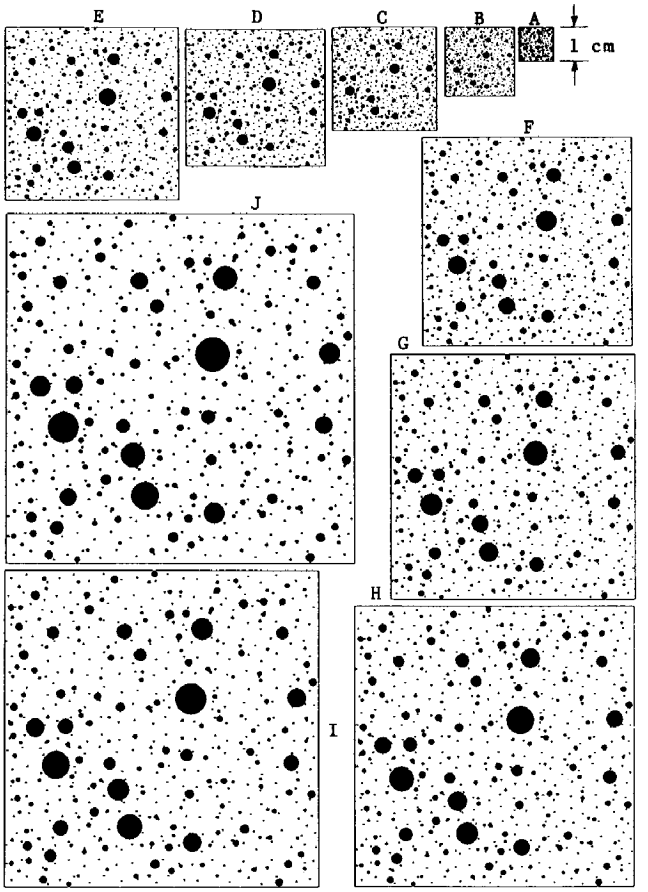

Figure 1–Mixed-speck images.

sizes randomly distributed throughout the image. The number of specks in each size was selected to obtain a nominal coverage of 10% for each image. The specks were not supposed to touch each other; but, the printed images contained quite a few touching specks.

3. Uniform speck size images. This set included four series of images which were made of uniform size specks. The first series consisted of 48 images. The images were printed in six square sizes resulting in image areas (A_i) of 100, 144, 196, 256, 324, and 400 mm, where, each A_i category consisted of eight images. They contained 13, 25, 38, 51, 63, 76, 89, or 100 specks to provide nominal speck area coverage ranging from 10.2 to 78.5%. Figure 2 shows a sample of the first series of images having different areas and speck counts of 13 to 51.

In the second series, speck diameters were reduced to 1/2 of those in the first (reference) series while the number of specks increased four times. Therefore, the nominal percent area coverage of the matching images remained constant (10.2 to 78.5%). The images in the third and forth series, respectively, had speck diameters of 1/4 and 1/8 and speck counts of 16 and 64 times compared to the first series. However, images requiring more than 832 specks could not be prepared due to memory limitation of the system. A sample of the images with nominally constant percent area coverage is shown in figure 3.

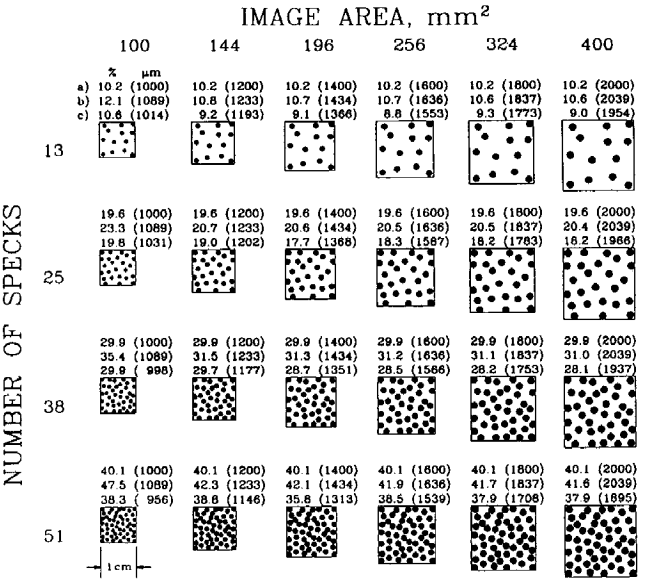

Figure 2–Sample of uniform speck size images with different area coverages—a) nominal; b) microscope; and c) image analysis data.

Imaging System

The imaging instrumentation included an Apple IIe-based system (Dapple Systems, Inc., Sunyvale, Calif.) with Imageplus+ software (Scientific Microprograms, Raleigh, N.C.), a Newvicon camera model WV 1550 (Panasonic Industrial Co., Secaucus, N.J.) with a Micro-NIKKOR 55 mm lens and, when required, a NIKKOR 2X teleconverter (Nikon, Inc., Melville, N.Y.). The images were digitized into 194 (vertical) × 254 (horizontal) pixels, with 64 grey

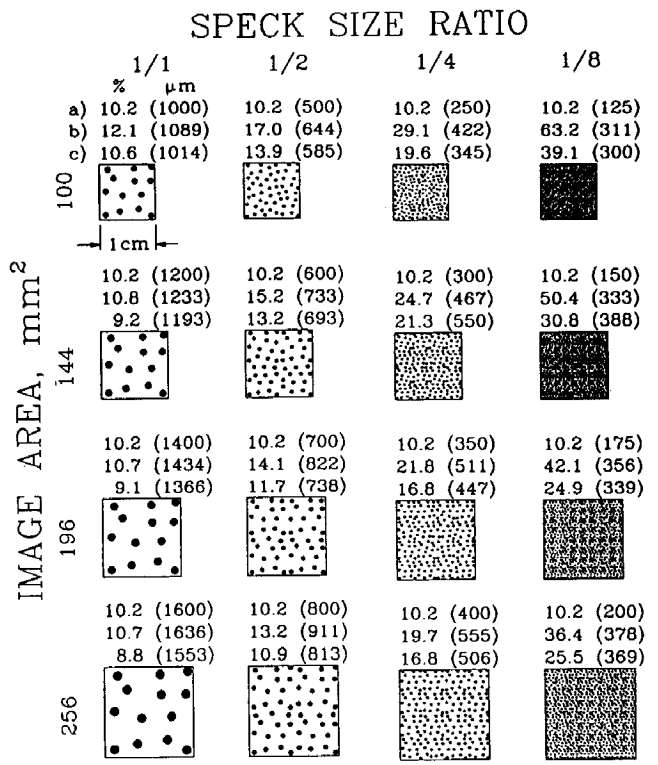

Figure 3–Sample of images with varying speck size ratios—a) nominal; b) microscope; and c) image analysis data.

levels. Upper and lower discriminator potentiometers allowed any combination of grey levels to be selected as threshold limits for forming binary images. Horizontal scan time was fixed so that the pixels were square. Room light was used to illuminate the images; some diffusion panels were used to improve lighting uniformity.

With this system, the smallest and largest horizontal dimensions that could be captured were about 6 and 47 mm, respectively, which correspond to resolutions of about 24 and 185 μm/pixel. The vertical dimension of field of view was 194/254 of the horizontal dimension. The software could count up to 254 specks per frame.

Microscope Measurements

Since the sizes of the printed specks differed from the nominal values, a microscope (Bausch & Lomb, Inc., Rochester, N.Y.) was used to obtain the actual measurements. An eyepiece gradicule, calibrated with a stage micrometer (with 13.5 μm divisions) was used to measure the length and breadth of the specks. Length was defined as the greatest dimension (major axis) of the speck and breadth was the dimension perpendicular to the length. Speck diameters were determined by averaging the length and breadth of each speck. For nominal speck diameters of 50 to 2000 μm, the single speck images (first set) were measured; for larger diameters, specks were selected from the mixed-speck images (fig. 1). The circularity of the specks was characterized as the ratio of breadth to length in the microscope measurements (table 1). Variability of the replications was expressed as the coefficient of variation (CV). The measurements were replicated eight times. A linear fit (LF) to the data provided the final adjustment and was used as the actual speck sizes in subsequent calculations (table 1). Area coverage was calculated from the LF speck size and the number of specks in the image.

Table 1. Speck size data

NL* (μm)	MS* (μm)	CV† (%)	LF* (μm)	IA* (μm)	CV† (%)	Circ‡ (%)	CV† (%)
50	275	9.2	244	282	0.9	71.2	8.8
100	274	6.0	289	294	0.9	83.0	6.1
150	354	5.0	333	352	2.4	75.3	7.8
200	345	5.1	378	351	1.3	73.0	7.4
250	432	5.6	422	453	1.4	81.2	3.6
300	499	4.3	467	497	0.7	74.8	5.2
350	496	3.7	511	508	1.1	82.0	1.3
400	548	3.3	555	555	1.3	87.7	1.5
450	595	2.2	600	599	1.4	81.0	4.5
500	630	3.3	644	646	1.2	88.6	4.8
550	691	3.3	689	677	1.0	89.1	3.7
600	706	2.3	733	717	0.8	91.9	2.3
650	763	2.5	778	754	1.2	81.1	6.3
700	792	3.9	822	780	1.5	93.6	1.8
750	892	2.8	866	881	1.0	93.9	3.2
800	936	2.8	911	913	1.1	84.8	3.3
850	948	4.2	955	949	1.0	96.6	2.0
900	1007	3.1	1000	991	1.1	98.3	1.3
950	1040	2.8	1044	1044	0.7	94.1	1.8
1000	1107	2.3	1088	1064	0.9	94.3	2.2
1100	1159	2.6	1132	1161	0.6	94.6	1.5
1200	1249	2.8	1233	1242	0.9	96.1	1.8
1300	1386	2.9	1333	1328	0.9	96.3	5.0
1400	1412	2.1	1434	1403	1.2	96.4	1.9
1500	1574	2.0	1535	1518	1.0	94.5	2.6
1600	1597	1.7	1636	1628	1.2	97.6	1.4
1700	1769	1.3	1736	1736	1.1	93.9	2.2
1800	1865	1.1	1837	1805	0.9	97.4	1.8
1900	1889	1.7	1938	1906	0.8	97.2	1.2
2000	2039	1.2	2039	1979	0.9	98.4	1.6

* Speck diameters: nominal (NL), microscope (MS), linear fit to microscope data (LF), and image analysis (IA).
† CVs refer to coefficient of variation of the preceding columns. The data for MS, IA, and Circ are means of 8, 3, and 8 replications, respectively.
‡ MS speck circularity = 100 × speck breadth / length.

Image Analysis

The field of view of the captured image was selected by moving the video camera farther from or closer to the target image. After the camera was positioned properly and focused on the desired target, image magnification was determined by placing a scale (with 0.1-mm divisions) horizontally across the field of view and adjusting vertical markers to a known distance.

One operator made all measurements with the imaging system. The operator trained by comparing speck sizes measured with the imaging system and using a gradicule eyepiece in the microscope. Another measure of the effect of the grey scale discriminator setting was to compare the grey scale image with the overlapped binary image on the system display. Using these comparisons it was found that speck sizes were measured fairly accurately. The lower grey scale discriminator was always set at zero or black, the upper scale was set at a level high enough to give a minimum of "white spots" in the images, yet low enough to eliminate isolated single pixel noise in the background. The same grey level was used for all images. The area measured is defined as the area of each pixel multiplied by the number of contiguous pixels in a spot. Speck diameters were calculated by assuming that the measured area was circular, i.e., $D = \sqrt{(4A/\pi)}$.

Each target image was measured three times; the imaging system was initialized for each replication. This involved adjusting the camera to a new focus on the image and recalculating the magnification for the image system. Because the captured image was rectangular, not all of the prepared target area could be included in a single measurement. The image width was adjusted to include as much of the target as possible without including the image frame line. When a frame contained less than 50 specks that touched, the touching specks were cut apart with single pixel lines (edited) to obtain improved discrimination.

Since no more than 254 specks could be counted in each frame and field of view was limited to a maximum horizontal dimension of 47 mm, the images in the mixed-speck set (fig. 1) were scanned differently. The 1 and 2 cm^2 images (fig. 1, A and B) were scanned into one image. The 3, 4, and 5 cm^2 images (fig. 1, C through E) were scanned into one image which was separated into quadrants for counting and sizing and total speck counts were combined into one file for each image. The larger images (fig. 1, F through J) were split into four frames (upper left, upper right, lower left, and lower right), and spots in each frame counted and stored in separate files. Specks in each image frame were grouped into 30 logarithmic ranges (with size ratios of 1.2 to 1.3) and speck count as well as the sum, average, and percent area coverage of each size range were determined.

Several statistical procedures (SAS, 1985) were used to analyze the data and make comparisons. The effects of the image area, speck size, and number of specks were

analyzed by the General Linear Model (GLM) procedure. The correlation between the variables were established with the Pearson Correlation Coefficient (PCC). The significance of the effects were expressed at the 95% confidence level.

Results and Discussion

Single Speck Sizes

Although the specks were made to exact size specifications (with Autosketch), the Laserjet printer did not print them as their nominal sizes (table 1). The very small specks were printed several times larger than nominal; however, the difference between the actual and nominal sizes decreased as the size of the speck increased. For a nominal size of 2000 μm, the difference amounted to about 2%. Variability of the measurements (CV), which reflects the variation among different prints and the measurement error, decreased as the size of the speck increased. Smaller specks were printed as an ellipse, but circularity increased as the diameter increased (table 1). Larger specks (> 2000 μm) were printed closer to their nominal sizes and more like perfect circles.

Speck diameters obtained with image analysis (column IA, table 1) were highly correlated with the linear fit (LF) to microscope measurements (PCC = 0.9993, $P < 0.01$). There was a 15.4% difference in the two diameters of the smallest speck (282 vs. 244 μm); otherwise, the differences were between −7.1 and +7.3%. Neither the differences between the actual and image analysis data nor the CVs of the latter showed any obvious trend.

Mixed-speck Images

Due to hardware and software limitations, only a portion of each full or quadrant image was captured in any imaging frame; therefore, the recorded number of specks were less than the expected count of 629 drawn with Autosketch (fig. 4). By normalizing the data (multiplying the counts by the ratio of image area to the scanned area), the counts were estimated for the full size of the images. The estimated (normalized) numbers did not agree with the expected count and revealed a pattern according to the size of the image. The numbers were underestimated for smaller images but increased as the image size increased. Underestimating the counts could mostly be attributed to touching of the specks. The system perceived the touching specks as one feature, resulting in significant underestimation of the counts for the three smallest images. The larger images had fewer touching specks and less error in counts, but this improvement was counteracted by errors associated with splitting the images into four quadrant frames. The partitioning lines could pass through a few specks dividing them into two or more pieces. Each fraction of a split speck could be read as a single speck resulting in overestimation of the counts. This probably was the main source of error in larger images. Another source of error may have been due to movement of the captured frame for each replication. The frames were moved so that the entire image was covered in three replications. This provided about 85% overlap between successive frames. Variability among replications (± standard deviation, s) is shown by vertical bars superimposed on the data points (fig. 4).

Figure 5 shows the smallest and largest speck diameters measured with the image analysis (IA) and microscope (MS), in the 1 to 10 cm^2 mixed-speck images (A through J). Regardless of the image area, image analysis undersized the smallest specks; but measured the largest specks closer to their actual sizes. In images "F" and "I", however, the partitioning line could have passed through the largest speck, split it into two or more pieces, and resulted in undersizing of the speck. The mean speck diameters, obtained from the microscope data (calculated-MS) and image analysis (measured-IA), are compared in figure 6. The measured mean was higher than the calculated mean for smaller images but the trend was also reversed for larger images. This may have been due to difference in the interpretation of speck boundaries in the measurements.

The percentage of speck area coverage is shown in figure 7. The calculated area coverage, obtained from the microscope data, was much higher than the nominal (10%) for the smaller images, however, it rapidly decreased as the image size increased, becoming close to the nominal value for the larger images. The image analysis data followed the same trend, but underestimating or overestimating the coverage without any obvious pattern. The variability in the measurements of the three replications, indicated by vertical lines (± s) showed more variable data for smaller

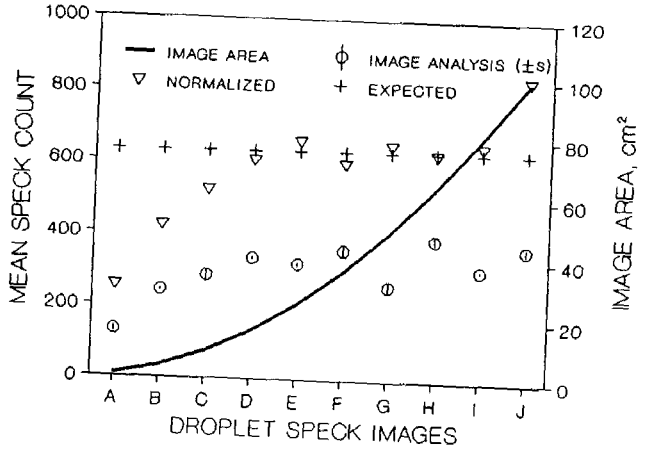

Figure 4–Speck counts of mixed-speck images.

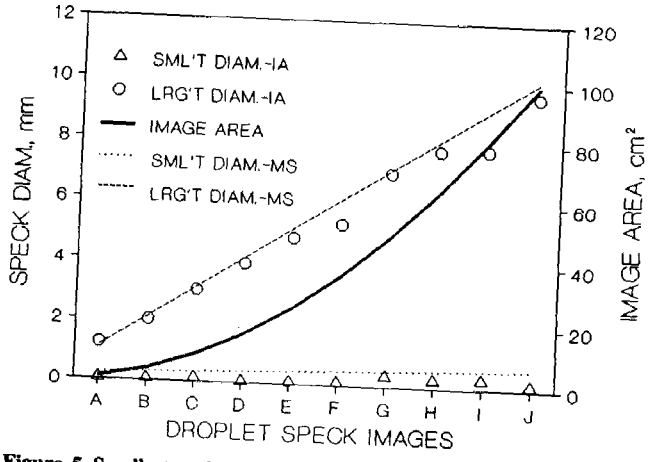

Figure 5–Smallest and largest speck diameters measured in mixed-speck images.

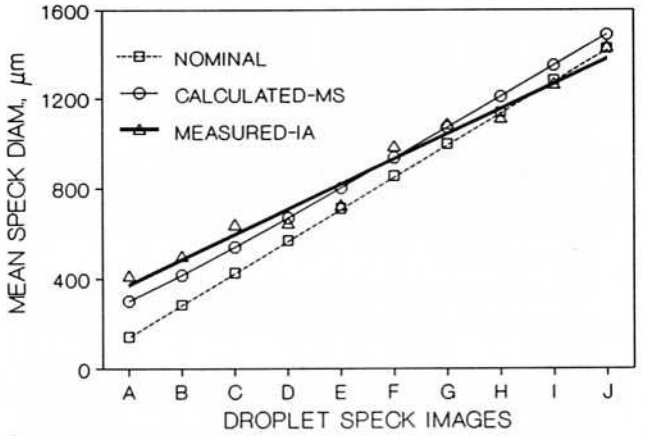

Figure 6–Comparison of mean speck diameters from microscope and image analysis measurements.

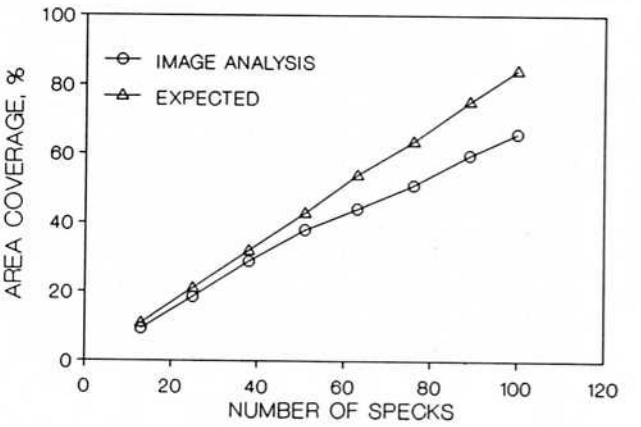

Figure 8–Percent area coverage vs. number of uniform size specks.

images. This variability may partially be explained by the mixed size of the specks, nonuniformity of the distribution patterns, and movement of the captured image frames. Sistler et al. (1982) also found that increasing the image size reduced the variations in readings, but decreased the accuracy of droplet size measurements and the percent area covered changed when the image was shifted as little as 1 cm.

Uniform Speck Size Images

The size and number of specks and the size of image area had significant effects on the measured area covered by the specks. In all images, the image analysis underestimated the percent area coverage as compared to the expected values (calculated from microscope measurements). The difference between the expected and image analysis values (error in image analysis) increased as number of specks increased (fig. 8). The error became much larger for more crowded images (fig. 9). This may partially have been due to contact of specks; although some touching specks were edited to increase discrimination in the measurements.

In general, as the size of image area increased, image analysis accuracy increased. Mean area coverage of figure 2 and figure 3 images are plotted in figures 10 and 11, respectively. The increase in the accuracy of area measurement for larger images could be attributed to decrease in contact of the specks and higher accuracy in sizing of the larger specks. Within each size of image area, reduction of the speck size (figs. 3 and 9) increased the error in area coverage measurement. Overall, there was a high correlation between expected and image analysis data (PCC = 0.9263, $P < 0.01$). The correlation became higher (PCC = 0.9942, $P < 0.01$) when only the 24 less crowded images (fig. 2) were used in the analysis.

Speck sizes obtained from image analysis were also affected by the speck count (fig. 2). Except for the lowest density images, the calculated speck size (from area coverage imaging) decreased as the number of specks increased; however, beyond about 40% coverage the sizing could no longer be reliable and the accuracy was adversely affected by touching of the specks.

It should be noted that the data were obtained by a single operator using a constant grey level setting and black and white contrast. These factors resulted in minimum variation among three replications. Image analysis of specks on leaves is more difficult because the leaf is not flat and creates focusing problems, droplets can wrap around veins, and leaves vary in color across the scanned area. Unless the software considers local grey

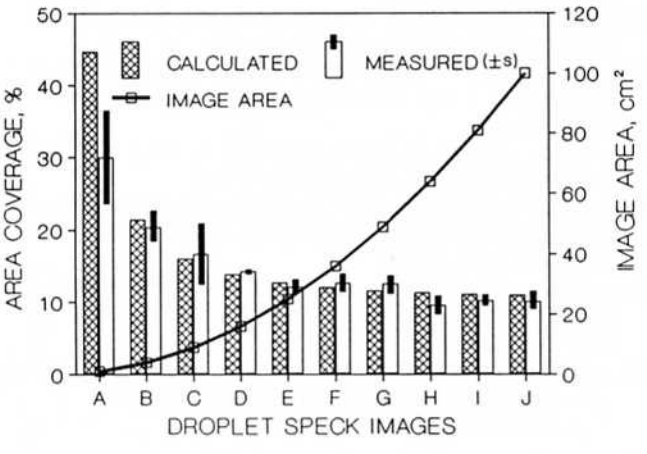

Figure 7–Area coverage measurements of the mixed-speck images.

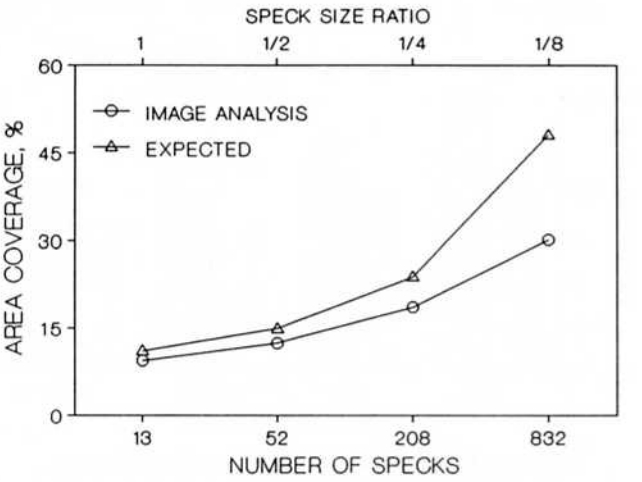

Figure 9–Percent area coverage vs. speck size ratio and number of specks.

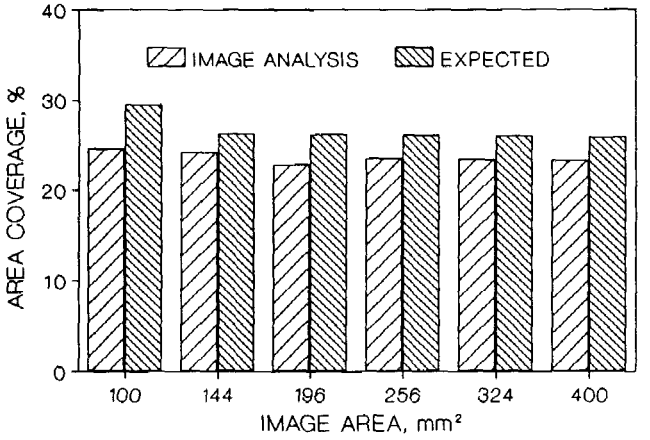

Figure 10–Mean percent area coverage of figure 2 images.

level gradient, then it becomes difficult to identify specks all over the leaf. Therefore, image analysis of spray droplet spots on leaf or other colored surfaces can be more variable and less accurate, although more representative of actual deposit. The resolution of the imaging could have direct impact on the accuracy of the measurements. Higher resolution systems such as the ones used by Panneton (1989), Sagi and Derksen (1991), and Evans et al. (1992) can potentially result in higher accuracies, particularly for speck size measurement.

The pixel resolution of the imaging system used here was low compared to systems currently available. However, the problems encountered with this system also apply to systems with higher resolutions if smaller-sized specks are considered. Droplets smaller than about 100 μm diameter are difficult to capture on collectors and often produce specks with low contrast that require special techniques to detect. This large class of small droplets will cause measurement problems with imaging systems regardless of resolution.

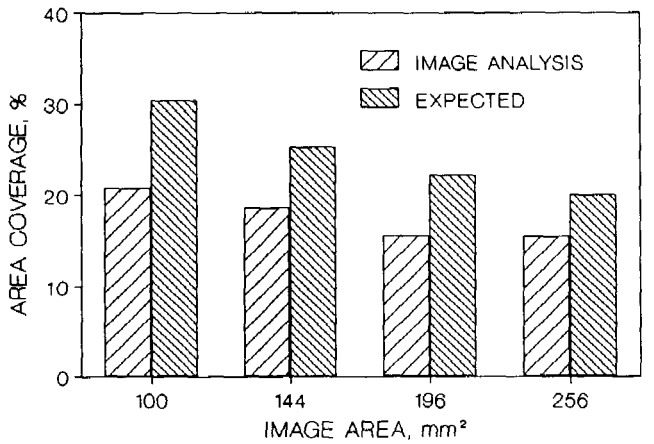

Figure 11–Mean percent area coverage of figure 3 images.

CONCLUSIONS

- The Laserjet printer did not accurately print small specks. The accuracy of printing a given diameter speck increased with speck diameter.
- The accuracy of image analysis for sizing single specks increased as speck size increased.
- The size of the image and the size and number of specks (within the image) had significant effects on speck sizing and percent area coverage measurements.
- The size and number of specks were not accurately measured for small and dense images made of small specks.
- Considering the large number of small droplets in agricultural sprays, deposit targets are likely to contain dense population of small droplets that may overlap. These targets require careful analysis methods to extract accurate droplet size measurement.

ACKNOWLEDGMENT. The authors wish to thank Roy D. Sweeb, Zhaohong Xian, and Keith Williams for their technical assistance.

REFERENCES

Brazee, R. D., O. K. Hedden and P. T. Keck. 1968. The USDA flying-spot particle analyzer. C. A. No. 53. Ag. Eng. Res. Div., USDA-ARS.

Byers, R. E., C. G. Lyons, Jr., K. S. Yoder and R. L. Horsburgh. 1984. Effects of apple tree size and canopy density on spray chemical deposit. *HortScience* 19(1):93-94.

Carlton, J. B. and L. F. Bouse. 1988. Exploring aerial spray sampling with a cylindrical collector. *Transactions of the ASAE* 31(4):990-997.

Edwards, G. J., W. L. Thompson, J. R. King and P. J. Jutras. 1961. Optical determination of spray coverage. *Transactions of the ASAE* 4(2):206-207.

Evans, M. D., S. E. Law and S. C. Cooper. 1992. Image analysis of particulate spray deposits using light intensified machine vision. ASAE Paper No. 92-7015, St. Joseph, Mich.: ASAE.

Franz, E. 1990. Progress towards a machine vision system for spray-deposit analysis: Software development. ASAE Paper No. 90-7515. St. Joseph, Mich.: ASAE.

———. 1992. A simple spray coverage analyzer. ASAE Paper No. 92-1617, St. Joseph, Mich.: ASAE.

Kranzler, G. A. and H. W. Downs. 1986. Machine vision analysis of granular chemical drift. ASAE Paper No. 86-1502, St. Joseph, Mich.: ASAE.

Liljedahl, L. A. and J. Strait. 1959. Spray deposits measured rapidly. *Agricultural Engineering* 40(6):332-335.

Maze, R. C. and K. T. Parekh. 1993. Sensor for measuring low volume spray deposit. ASAE Paper No. 93-1002. St. Joseph, Mich.: ASAE.

Panneton, B. 1989. A system for analyzing spray samples. ASAE Paper No. 89-0017. St. Joseph, Mich.: ASAE.

Sagi, Z. and R. C. Derksen. 1991. Detecting spray droplets on leaves with machine vision. ASAE Paper No 91-3050. St. Joseph, Mich.: ASAE.

Salyani, M. and C. W. McCoy. 1989. Spray droplet size effect on mortality of citrus rust mite. ASTM STP 1036. *Pest. Form. and Appl. Sys.* 9:262-273.

Salyani, M. and J. Serdynski. 1990. Development of a sensor for spray deposition assessment. *Transactions of the ASAE* 33(5):1464-1468.

Salyani, M. and J. D. Whitney. 1988. Evaluation of methodologies for field studies of spray deposition. *Transactions of the ASAE* 31(2):390-395.

SAS Institute, Inc. 1985. *SAS User's Guide: Statistics*. Version 5 Ed. Cary, N.C.: SAS Institute, Inc.

Sistler, F. E., P. A. Smith and D. C. Rester. 1982. An image analyzer for aerial application patterns. *Transactions of the ASAE* 25(4):885-887.

Staniland, L. N. 1959. Fluorescent tracer techniques for the study of spray and dust deposits. *J. Agric. Eng. Res.* 4(2):110-125.

Ware, G. W., B. J. Estesen, W. P. Cahill, P. D. Gerhardt and K. R. Frost. 1969. Pesticide drift. I. High-clearance vs. aerial application of sprays. *J. Econ. Ent.* 62(4):840-843.

Whitney, R. W. and L. O. Roth. 1985. String collector for spray pattern analysis. *Transactions of the ASAE* 28(6):1749-1753.

Yates, W. E., N. B. Akesson and R. E. Cowden. 1974. Criteria for minimizing drift residues on crops downwind from aerial applications. *Transactions of the ASAE* 17(4):627-632.